2

Characterization and Probabilistic Modeling of Heterogeneous Media

François WILLOT
Mines ParisTech, Paris, France

2.1. Introduction

The fine structure of metals, composites and other materials, examined under a microscope, depends on the scale at which it is viewed. A typical example is concrete, which at smaller scales consists of mortar, aggregates and cement (Stroeven 2000). In most cases, such a microstructure appears as a random arrangement, in space, of "phases", namely of its different constituents at the scale under consideration. As noted by Matheron (1967), behind the multiplicity of shapes and sizes, and the variety of network of interstices between aggregates and clusters of particles, these random arrangements also have a repetitive character (see Figure 2.1). Random set theory, whose modern developments originate in the works of Choquet (1954), Matheron (1965) and Kendall (1974), aims to quantify and simulate the morphology of heterogeneous media using probabilistic methods. Reconsidering the example of concrete, the forms of aggregates present in such materials are always different from one another. However, they present specific characteristics such as their granulometry (Escoda *et al.* 2015). It is therefore natural to study whether it is possible, by means of a limited number of "morphological" descriptors, to model accurately a given microstructure, seen as the realization of a random set (Molchanov 2005), with the aim of predicting its mechanical properties, in particular by homogenization (Milton 2002).

Mechanical Engineering under Uncertainties,
Christian GOGU.

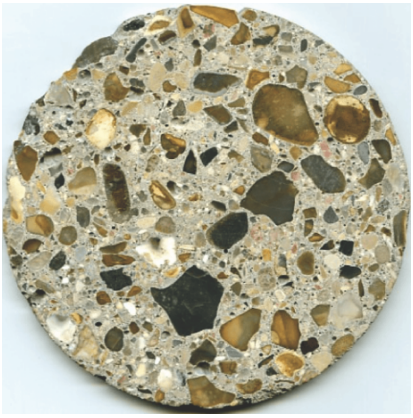

Figure 2.1. *"Biloba" concrete core, according to Escoda (2012) (source: EDF). For a color version of this figure, see www.iste.co.uk/gogu/uncertainties.zip*

The first question, addressed in this chapter, is the subject of integral geometry (or stochastic geometry) developed by Matheron (1975) and Kendall (1974), among others. Two main problems arise. First, the development of morphological criteria to quantify the shape of objects and their distribution in space. These criteria make use of image transformations, which are most often nonlinear operators derived from mathematical morphology (Matheron and Serra 1982). These methods apply to random sets or functions that can be very general, for example tensor-valued ones (Angulo 2012), such as a strain or stress field. The second problem is the simulation of random microstructures representative of real structures based on morphological criteria. Probabilistic models of structures, some of which relying on analytical tools, provide means to define and simulate representative random realizations of real microstructures. Among numerous examples, the following works can be cited: Greco *et al.* (1979), Jeulin *et al.* (1995), Redenbach *et al.* (2011) and Bortolussi *et al.* (2018).

This chapter is organized as follows. Section 2.2 is dedicated to the main theoretical and numerical tools for characterizing microstructures from two- or three-dimensional images. Random point processes are introduced in section 2.3, Boolean models in section 2.4 and repulsion models in section 2.5. The main random partition models are introduced in section 2.6 and random structures from Gaussian fields are briefly discussed in section 2.7. The chapter is concluded by section 2.8.

2.2. Probabilistic characterization of microstructures

2.2.1. *Random sets*

A random set is a stochastic model whose realizations are sets of $\mathbb{R}^d$ (where d = 2 or 3 is the dimension). For reasons that will be explained later, we are interested in closed sets comprised in $\mathbb{R}^d$. The distribution of a random set is completely specified by a probability measure defined on a σ-algebra, that is, a space containing $\mathbb{R}^d$, the empty set, and which is stable by a countless number of unions and intersections. This algebra is used to define measures on sets of $\mathbb{R}^d$. These definitions are discussed by Lantuéjoul (2002, Chapter 2).

A fundamental theoretical tool enabling random-orthogical sets to be characterized is the Choquet capacity. It can be written as follows:

$$T(K) = P\{X \cap K \neq \varnothing\} \qquad [2.1]$$

where K is a compact set of $\mathbb{R}$ and X a realization of a random set. It satisfies the following properties:

i) $0 \leq T(K) \leq 1$ for any compact subset K, and $T(\varnothing) = 0$ $T(\mathbb{R}^d) = 1$;

ii) for $T(K) \leq T(K \cup K')$ all compact subsets K and K';

iii) if K_n is a sequence of decreasing compact subsets (as inclusion defines it) in $\mathbb{R}^d$ with the limit $\mathcal{K}$, then:

$$\lim_{n\to\infty} T(K_n) = T(\mathcal{K})$$

The "hitting functional" T can be seen as a generalization of the cumulative distribution function for random sets (Matheron 1975). This interpretation is justified by the following theorem (Choquet 1954; Kendall 1974; Matheron 1975):

THEOREM 2.1.– Let T be a functional defined on the set of compacts subsets $\mathbb{K}$ of $\mathbb{R}^d$. Then there exists a single probability measure P defined on the σ-algebra $\mathbb{F}_K$ such that:

$$P(\mathbb{F}_K) = T(K)$$

if, and only if, T is a Choquet capacity verifying (i), (ii) and (iii) above.

The σ-algebra $\mathbb{F}_K$ is the smallest σ-algebra containing the closed sets that meet the compact subsets of $\mathbb{R}^d$

$$\mathbb{F}_K = \{F \in \mathbb{F} : F \cap K \neq \varnothing\}, \qquad K \in \mathbb{K} \tag{2.2}$$

where $\mathbb{F}$ is the set of the closed subsets of $\mathbb{R}^d$ and $\mathbb{K}$ the set of the compacts subsets.

The realizations of the random set are in $\mathbb{F}$, that is, in the closed set. This restriction comes from the fact that the functional $T(K)$ does not allow distinguishing a set from its closure. Note that there exists a dual theory involving the open sets of $\mathbb{R}^d$ (Lantuéjoul 2002). However, it is generally preferable to work on closures, because they include random point or line processes that are very important for a large number of models.

When restricted to a finite set of points, the functional $T(K)$ defines the *spatial distribution* of the random set X. If K is a finite set of n points:

$$T_n(x_1,...,x_n) = P\{x_i \in X, 1 \leq i \leq n\} \tag{2.3}$$

The spatial distribution does not allow us to fully characterize X. For example, if X is itself a finite set of points, it is clear that $T_n \equiv 0$ for every $n \geq 0$. On the other hand, the spatial distribution makes it possible to define a single random set, which is a minimizer of $T(K)$; see on this subject the works of Matheron (1975).

DEFINITION 2.1.– *A random set is said to be stationary if its Choquet capacity $T(K)$ is translation invariant of K, that is*:

$$T(K) = T(K_x), \qquad K_x = \{k + x; \quad k \in K\} \tag{2.4}$$

Moreover, if the values $T(K)$ taken by the functional remain unchanged after a rigid body movement of K, including rotations, the random pattern is said to be isotropic.

It is assumed in the following that X is a stationary, ergodic random set. There are several definitions of ergodicity in the literature, one of the most general being given by Heinrich (1992). This definition, which is somewhat technical, is not detailed here.

Intuitively, ergodicity implies that the Choquet capacity $T(K)$ can be calculated from a single realization X on $\mathbb{R}^d$ and more precisely from the average density of the set:

$$\{x \in \mathbb{R}^d : K_x \cap X \neq 0\} \quad [2.5]$$

In such a case, for example, the density of X (volume or surface area fraction), calculated over a sufficiently large domain, is no longer asymptotically a random variable. This property is in line with a more operational definition of ergodicity proposed by other authors (Lantuéjoul 1991). In practice, the Choquet capacity is calculated based on a large-sized realization X using:

$$T(K_x) = P\{K_x \cap X \neq \varnothing\} = P\{x \in X \oplus \check{K}\} \quad [2.6a]$$

$$X \otimes \check{K} = \{x - k,\, x \in X,\, k \in K\} \quad [2.6b]$$

operators $\oplus$ and $\check{}$ defining morphological dilation, in this case applied to X by a structuring element K (Serra 1980). The operator $\oplus$ is the Minkowski addition:

$$K \oplus K' = \{x + x';\, x \in K, x' \in K'\} \quad [2.7]$$

Random set theory has been extended by Matheron (1969) to upper or lower semicontinuous random functions $Z(x)$ ($x \in \mathbb{R}^d$). Indeed, if for example $Z(x)$ is upper semicontinuous, the supergraph:

$$\{(x, z) \in \mathbb{R}^d \times \mathbb{R} : \; Z(x) \geq z\} \quad [2.8]$$

is a random set in $\mathbb{R}^{d+1}$ (Lantuéjoul 2002).

Tensor (or "spectral") valued functions require more sophisticated mathematical morphology tools (Angulo 2012). Random sets can also be defined on non-ordinary topological sets such as point clouds, random trees. These theories are not discussed in this chapter.

2.2.2. *Covariance*

In the event that K is a bipoint, the functional $T(K)$ is the covariance of the set X.

DEFINITION 2.2.– *The covariance of the random set* X *is the function defined on* $\mathbb{R}^d \times \mathbb{R}^d$

$$C(x, x+h) = P\{x \in X, x+h \in X\}, \quad x, h \in \mathbb{R}^d \qquad [2.9]$$

When X *is stationary, we have* $C(x, x+h) = C(h)$. *The correlation function is denoted as* $\rho(h) = C(h)/C(0)$.

Moreover, it is clear that $C(h)$ only depends on the norm of h in the case of an isotropic random set. The covariance is estimated from a realization of an ergodic stationary set by:

$$C(h) = P\{x \in X \cap X_{-h}\} = V(X \cap X_{-h}) \qquad [2.10]$$

where $V(\cdot)$ designates the mean density (area or volume fraction) of the set being considered.

NOTE.– The covariance provides access to statistical information on the set X, in particular (Matheron 1975; Lantuéjoul 2002):

i) $C(0) = V(X)$;

ii) $\lim_{|h| \to \infty} C(h) = C(0)^2$;

iii) $C_{X^c}(h) = 1 - 2C(0) + C(h)$, where C_{X^c} is the covariance of the complement of X.

The quantity in (i) is the volume or surface fraction of the set X, property (ii) is obtained if the two events $x \in X$ and $x+h \in X$ are asymptotically independent, when $h \to \infty$. This property is valid for an ergodic stationary ensemble. It does not hold if, for example, the set X is periodic (in this case, the covariance is itself a periodic function). Finally, property (iii) shows that the covariance of a set and its complement can be inferred from one another.

In addition, the specific area ($d = 3$) or perimeter ($d = 2$) $|\partial X|$ of X are given by:

$$|\partial X| = -\frac{1}{\omega_{d-1}} \int_{S_d} \mathrm{d}\alpha \left. \frac{\partial C(h)}{\partial h} \right|_{h=0} \qquad [2.11]$$

where the sum is carried out on all the angular sectors of the unit sphere S_d in dimension d, and ω_{d-1} designates the volume of the unit ball of dimension $d-1$. Therefore, in dimension $d = 2$ and 3:

$$S_V(X) = -\frac{1}{\pi}\int_{S_3} \mathrm{d}\alpha \left.\frac{\partial C(h)}{\partial h}\right|_{h=0} \qquad [2.12a]$$

$$P_S(X) = -\frac{1}{2}\int_{S_2} \mathrm{d}\alpha \left.\frac{\partial C(h)}{\partial h}\right|_{h=0} \qquad [2.12b]$$

S_V designates the specific surface area (surface density of the boundary X) and P_S the specific perimeter. Both are expressed in inverse length unit. It should be noted that in an isotropic model with $\partial C(h)/\partial h = +\infty$ in $h = 0$, the specific surface area is then infinite (for a fractal object). More precisely, a power law behavior $C(h) \sim h^{\beta}$ can be related to the origin when $h \to 0$ ($0 < \beta < 1$) with the fractal dimension (Hausdorff dimension) of the surface $d_s = 3 - \beta$ (Matheron 1989b).

The covariance function provides access to other types of information. For example, inflection points can reflect the presence of nested structures or clusters, the values $C(h) < C(0)^2$ of anticorrelation phenomena. The latter appear in particular in inclusion matrix-based models in which interpenetration between particles is prohibited.

Other properties relate to the second derivative of the original variogram. It is infinite in absolute value when the surface of the random set presents a cusp, with finite probability within a bounded domain. In the case of angular points, the second derivative is finite. It is finally zero if the surface is regular (Emery and Lantuéjoul 2011).

NOTE.– Covariance functions are not arbitrary. In particular, they are definite positive or more precisely:

$$\sum_{\alpha,\beta=1}^{n} \lambda_\alpha \lambda_\beta C(x_\alpha - x_\beta) \geq 0 \qquad [2.13]$$

for any sequence of points x_α and any finite sequence of real numbers λ_α ($\alpha = 1$, ..., n).

The Bochner theorem shows that the above property is verified if and only if the covariance is the Fourier transform of a positive measure (Bochner 1959; Christakos 1984). In the case of a homogeneous random function $Z(x)$ whose autocovariance function is written as:

$$\chi(h) = \langle [Z(x) - \mu][Z(y) - \mu] \rangle, \qquad \mu = \langle Z(x) \rangle \qquad [2.14]$$

It is then showed that (Torquato 2013):

$$\widetilde{\chi}(k) = \int_{\mathbb{R}^d} \mathrm{d}r \, \chi(r) e^{-ik \cdot r} \geq 0 \qquad [2.15]$$

for every k, as soon as χ is integrable, that is:

$$\int_{\mathbb{R}^d} \mathrm{d}r |\, \chi(r) \,| \leq \infty$$

NOTE.– The above property applies to random functions. However, it does not make it possible to fully characterize functions that are covariances of random *sets*. A counterexample is given by Torquato (2013).

2.2.3. *Granulometry*

Granulometries are defined using a family of operators Φ_λ depending on a length parameter. The properties of this increasing, anti-extensive and idempotent operator were introduced by Matheron (1975). In practice, a convex set K and a family of sets λK ($\lambda > 0$) obtained by homothety are considered, which are used as parameters for the operator Φ.

In the case of opening granulometry, the operator Φ_λ is written as:

$$\Phi_\lambda(X) = (X \ominus K) \oplus \lambda K \qquad [2.16]$$

where $\ominus$ is the Minkowski subtraction:

$$K \ominus K' = \{x - x'; x \in K, x' \in K'\} \qquad [2.17]$$

such that Φ_λ is an opening through the structuring element K. Similarly, a closing can be defined $\Phi_\lambda(X) = (X \oplus K) \ominus K\lambda$

Erosions or dilations by λK also define granulometries. In practice, however, they are less sensitive to microstructure than openings and closings (Escoda *et al.* 2015) and are therefore less frequently used.

2.2.4. *Minkowski functionals*

We examine the set $\mathcal{C}^d$ of convex compacts subsets of $\mathbb{R}^d$ and the real-valued functionals $\Phi(K)$ defined in $\mathcal{C}^d$.

The following properties are defined:

DEFINITION 2.3.– *The functional ϕ defined on $\mathcal{C}^d$ is:*

– isometry invariant if for any isometry $\mathcal{G}$ (translation, rotation, reflection, etc.) and compact convex subset K, $\Phi(\mathcal{G}K) = \Phi(K)$;

– monotonic for inclusion if $K_1 \subseteq K_2 \Phi(K_1) \leq \Phi(K_2)$;

– C^d-additive if for any pair of convex subsets K_1, K_2 such that $K_1 \cup K_2 \in \mathcal{C}^d$, $\phi(K_1 \cup K_2) = \phi(K_1) + \phi(K_2) - \phi(K_1 \cap K_2)$.

The following theorem is due to Minkowski:

THEOREM 2.2.– The isometrically invariant, monotonic and C ^{d}-additive functions are positive linear combinations of $d+1$ functions known as homogeneous Minkowki functions of degrees W_i, that is verifying $d-i$:

$$\lambda > 0 W_i(\lambda K) = \lambda^{d-i} W_i(K)$$

By convention, Minkowski's functionals all take the same value in the unit ball in dimension d.

NOTE.– Let us take a closer look at the cases $d = 2$ and $d = 3$. We have:

– $W_0(K) = | K |$ the volume ($d = 3$) or the surface area ($d = 2$) of K;

– $W_1(K) = | \partial K | / d$, where $| \partial K |$ is the length ($d = 2$) or area ($d = 3$) of the boundary of K;

– $W_{d-1}(K) = \omega_d \gamma(K)/2$ where $\gamma(K)$ designates the average extension of K. If $\gamma(K,v)$ is the extension of K in the direction v (the length of the projection of K on a straight line of direction v), then:

$$\gamma(K) = \frac{\int_{v \in S_d} \mathrm{d}v \gamma(K,v)}{\int_{v \in S_d} \mathrm{d}v}$$

– $W_d(K) = \omega_d$ if $K \neq \varnothing$, and 0 otherwise.

Thereby, for $d = 2$:

$$b(K) = \frac{1}{\pi} |\partial K|$$

When $d = 3$, W_2 is proportional to the integral of the mean curvature:

$$M(K) = \int_{\partial K} \mathrm{d}S m(x)$$

$$m(x) = \frac{1}{2}\left(\frac{1}{R_1} + \frac{1}{R_2}\right) \qquad [2.18]$$

where $R_1(x)$, $R_2(x)$ are the radii of curvature in x on the surface of the convex.

Steiner's formula can be used to connect the volume of the dilation of a convex set K by a ball $B(0,r)$ of radius r, knowing the Minkowski functionalities of K.

THEOREM 2.3.– Let $K \in \mathcal{C}^d$ and $r > 0$. The volume of the dilated set of K by the ball of radius r is:

$$|K \oplus B(0,r)| = \sum_{j=0}^{d} \binom{d}{j} W_j(K) r^j \qquad [2.19]$$

where $\binom{d}{j}$ designates the binomial coefficient in d, j.

2.2.5. *Stereology*

An affine space A_i of dimension $i < d$ cuts the convex set K into a convex subset $A_i \cap K$. An affine space of dimension i is denoted by $\mathcal{A}_i$ taken uniformly among all those that cut K. The Crofton formula (Hadwiger 1957) gives the average of the Minkowski functionals of $A_i \cap K$ (where $A_i \in \mathcal{A}_i$) as a function of those of K.

THEOREM 2.4.– The Minkowski functionals $W_j^{(i)}$ of the intersection of $K \in \mathcal{C}^d$ with an affine space of dimension $i < d$ are written as:

$$E\left\{W_j^{(i)}(K \cap A_i)\right\}_{A_i \in \mathcal{A}_i} = \frac{\omega_i \omega_{d-j}}{\omega_{d-i}\omega_{i-j}} \frac{W_j(K)}{W_i(K)}, \qquad 0 \le j < i \qquad [2.20]$$

Given that isotropy and stationarity are assumed, these properties allow one to calculate the volume of 3D objects based on a two-dimensional slice assumed to be representative, or to infer the surface area of these objects from an estimate of the perimeter on a slice (Schneider and Weil 2008).

2.2.6. *Linear erosion*

Instead of calculating the Choquet capacity for a compact subset reduced to a bi-point (or n points), it is now chosen to be applied to a segment L of length h and orientation α. This is obtained by linear erosion:

$$X \ominus L = \bigcap \{X - u : u \in [0;h]\} \qquad [2.21]$$

For a stationary set, the moment is defined by linear erosion $P(h)$ of X using the Lebesgues measure of $X \ominus L$:

$$P(h) = |X \ominus L| = P\{L \subset X\} \qquad [2.22]$$

The following properties are easily verified:

– $P(0) = C(0)$ is the volume (or surface) fraction of the set X;

– the linear erosion moment and the covariance have the same slope at the origin, namely $P'(0) = C'(0)$;

– for a fixed angle α, $C(h) \geq P(h)$;

– at a fixed angle α, $P(h)$ is a decreasing function of h;

– $P(\infty) = 0$.

In addition, the opening granulometry of a segment L can be characterized by:

$$P\{x \in X \circ L\} = P(h) - hP'(h), \qquad X \circ L = (X \ominus L) \oplus L \qquad [2.23]$$

where $P'(h)$ is the derivative of $P(h)$.

2.2.7. *Representative volume element*

We consider a measure of the volume fraction of an ergodic random set X, estimated from a realization in a bounded domain:

$$f_V = \frac{1}{|V|}\int_V 1_X(x)\mathrm{d}x \qquad [2.24]$$

DEFINITION 2.4.– *The integral range of the ergodic random set X is the d-volume quantity:*

$$A_d = \int_{\mathbb{R}^d} \mathrm{d}h \frac{C(h) - C(0)^2}{C(0) - C(0)^2} \qquad [2.25]$$

It is shown that if X is of finite integral range A_d, the variance of the estimates f_V of f varies asymptotically as (Matheron 1989a):

$$\mathbb{E}\{(f_V - f)^2\} = \frac{\sigma^2 A_d}{|V|} + \mathcal{O}\left(\frac{1}{|V|}\right), \qquad |V| \to \infty \qquad [2.26]$$

where the volumes V are increasing compacts that asymptotically overlap $\mathbb{R}^d$. Furthermore, the above equation provides a good estimate of the variance when $|V| \gg A_d$. This relation shows that the volume V behaves as $n = |V|/A_d$ volume-independent domains of integration range. In the case where $A_d = +\infty$ that is when

the quantity is $C(h)-f^2$ not infinitely integrable, the asymptotic relation [2.26] is no longer valid. This is particularly the case for models containing Poissonian varieties of infinite size, in which correlations exist at scales as large as desirable (Lantuéjoul 1991; Jeulin 2016). Exact results for the asymptotic behavior of the variance of f_V of some cylinder Boolean structures are given by Willot (2017). For three-dimensional Boolean fibrous materials containing large-sized elongated particles, for example, two regimes appear. The variance of the estimates f_V behaves as $\sim 1/|V|^{2/3}$ in a domain $h \ll \ell$ and as $\sim 1/|V|$ when $h \gg \ell$, the change of regime occurs over the length $h \approx \ell$ of the fibers.

Mechanical fields (for example, the strain tensor) can also be associated with an integral range; by studying the asymptotic behavior of the average field over subvolumes, this average reflecting the apparent properties is (for example, the apparent elastic modulus) associated with a finite size volume (Altendorf *et al.* 2014). Azzimonti *et al*. (2013), for example, numerically calculates separate exponents for the microstructure and the displacement field (in optics) of a repository model.

2.3. Point processes

A random point process is defined as a random set of points each realization of which is a closed set that contains a finite or countable number of points. In general, it is assumed that each realization is locally finite, that is, the number of points contained in a compact set is almost surely finite.

Random point processes are a very rich class of stochastic models. They are useful as well for defining models of continuous random sets. For example, a straight line in the plane can be represented by an angle, measured with respect to a fixed axis, and a positive real, its distance to a fixed point. A process of random points in a semi-infinite band $[0;2\pi]\times\mathbb{R}_+$ consequently corresponds to a random process of straight lines.

In the case of a Poisson point process (that will be defined below), a pattern of Poissonian lines is obtained (see Figure 2.2(f)). Similarly, a random point process can be used as germs for Boolean schemes (see Figures 2.2(a) and (b)) or for a dead-leaves model (see Figure 2.2(c)) or random partitions (see Figures 2.2(d) and (e)).

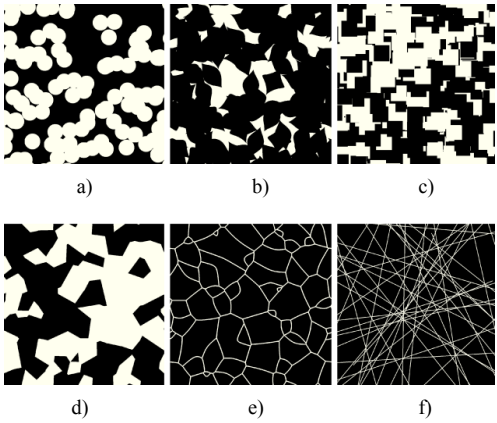

Figure 2.2. *Examples of stochastic models derived from random point processes: (a and b) Boolean models; (c) dead-leaves model; (d) labeling of a Poisson–Voronoi random partition; (e) Johnson–Mehl random partition; (f) Poisson line processes. For a color version of this figure, see www.iste.co.uk/gogu/uncertainties.zip*

The remainder of this section focuses exclusively on Poisson point processes. The reader is referred to Van Lieshout (2000) and Daley and Vere-Jones (1988) for a description of other random point processes.

2.3.1. *Homogeneous Poisson points processes*

Let X be a realization of a random point model and $T(K)$ its Choquet capacity. We consider the spatial distribution:

$$P_K(n) = P\{N(K) = n\}, \qquad n \geq 0$$

defined for any compact set K and integer n, with $N(K)$ the "count function", namely the function that assigns with K the number of points of X contained in K. The Choquet capacity is by the way written as $T(K) = 1 - P_K(0)$.

It is natural to assume that in a compact set δK of infinitesimal volume, the probability that a point is included in δK is of the order of the volume of δK:

$$\lim_{|\delta K|\to 0} T(\delta K) \propto |\delta K| \qquad [2.27]$$

Subsequently, it is assumed that:

$$\lim_{|\delta K|\to 0} T(\delta K) = \theta |\delta K| \qquad [2.28]$$

for any series of compact sets δK of volume tending toward 0 containing a point, where θ (with unit the inverse of a *d*-volume) is a constant. The parameter θ is the *intensity* of the Poisson point process and designates a point density (number of points per unit of *d*-volume).

DEFINITION 2.5.– *A homogeneous Poisson point process of intensity* $0 < \theta < \infty$ *is a point process verifying [2.28] and such that the events* $K \cap X \neq \varnothing$ *and* $K' \cap X \neq \varnothing$ *or* K *and* K' *included in* $\mathbb{R}^d$ *are independent as soon as* K *and* K' *are disjoint.*

Let us calculate the spatial distribution of a homogeneous Poisson point process of intensity θ. Consider a compact set K that we partition into N subdomains of infinitesimal volume $|\delta K| = |K|/N$:

$$P_K(n) = (\theta |\delta K|)^n (1 - \theta |\delta K|)^{N-n} \frac{N!}{n!(N-n)!} = \frac{\theta^n |K|^n e^{-\theta|K|}}{n!} \qquad [2.29]$$

after using the Stirling $z! = z^z e^{-z}\sqrt{2\pi z}$ formula. According to [2.29], the spatial distribution of the point process is therefore, of fixed K, a Poisson distribution of mean $\theta |K|$, hence the name *Poisson point process*. Moreover, it is clear that:

$$T(K) = 1 - e^{-\theta|K|} \qquad [2.30]$$

Using [2.29], the probability of simultaneous events involving N can be calculated such that:

$$P\{N(K) = n, N(K') = n'\}$$

$$= \sum_{i=0}^{n'} P\{N(K \cap K') = i\} P\{N(K \setminus K') = n - i\} P\{N(K' \setminus K) = n' - i\}$$

for any pair of compact set K, K' with $n' \leq n$. A similar general formula can be used to calculate the probability of the event $(N(K_1) = n_1) \cap \ ... \ \cap (N(K_N) = n_N)$ for $K_i \in \mathbb{K}$, $n_i \geq 0$, $N \geq 1$.

NOTE.– Most authors define a Poisson point process as a spatial distribution process [2.29] and such that $N(K)$ and $N(K')$ are independent random variables for disjoint K and K' (see, for example, Lantuéjoul 2002).

THEOREM 2.5.– Let us assume that $N(K) = n$ in a certain domain K. Based on property [2.28], the n points are uniformly distributed in K and it can be shown that:

$$P\,P\{N(K') = n' \mid N(K) = n\} = \binom{n}{n'} \left(\frac{|K'|}{|K|}\right)^{n'} \left(1 - \frac{|K'|}{|K|}\right)^{n-n'} \qquad [2.31]$$

for $K' \subset K$, $n' \leq n$. Therefore, to simulate a Poisson process in a finite volume domain K, one simply has to randomly draw an integer n according to the probability distribution [2.29], then to implant n points uniformly in K.

2.3.2. *Inhomogeneous Poisson point processes*

In an inhomogeneous Poisson point process, the density θ is now a function of x:

$$\lim_{|\delta K(x)| \to 0} T(\delta K(x)) = \theta(x)\,|\,\delta K(x)\,| \qquad [2.32]$$

where the $\delta K(x)$ are a sequence of volume compact sets tending to 0 and containing the point x. One further defines:

$$\theta(K) = \int_K \mathrm{d}x \theta(x) \qquad [2.33]$$

As with a homogeneous Poisson point process, the random variables $N(K)$ and $N(K')$ are independent if the compact sets K and K' are disjoint.

Equation [2.29] then remains valid, provided $\theta\,|\,K\,|$ is replaced by $\theta(K)$:

$$P_K(n) = \frac{\theta^n(K) e^{-\theta(K)}}{n!} \qquad [2.34]$$

which is still a Poisson distribution. Similarly, we have:

$$T(K) = 1 - e^{-\theta(K)} \qquad [2.35]$$

NOTE.– In the case where the intensity $\theta(x)$ is a random, locally integrable function, a Cox process is obtained (Lantuéjoul 2002). This random point process is not a Poisson point process, since $N(K)$ is not generally a random Poisson variable (see Lantuéjoul (2002) for examples of non-Poisson distributions). A relevant example of a Cox process is obtained when $\theta(x)$ is the indicator of a random set, which allows the construction of multiscale sets (Jeulin and Ostoja-Starzewski 2001; Willot and Jeulin 2011).

2.4. Boolean models

2.4.1. *Definition and Choquet capacity*

The Boolean model is based on two fundamental components:

– a random Poisson point process of intensity $\theta(x)$ (see section 2.3);

– a family $A(x)$ ($x \in \mathbb{R}^d$) of random non-empty compact sets included in $\mathbb{R}^d$.

They are used in the following definition:

DEFINITION 2.6.– *The Boolean model of intensity θ associated with the family* $(A(x))$ *is the union of all the compact sets* $A(x)$ *implanted on the germs of a Poisson point realization* $\mathcal{P}$ *of intensity* θ*:*

$$X = \bigcup_{x \in \mathcal{P}} A(x) \qquad [2.36]$$

THEOREM 2.6.– Now let K be a compact set of $\mathbb{R}^d$ and X a Boolean model of primary grain A and intensity θ. The number $N(K)$ of primary grains intersected by K follows a Poisson distribution of parameter $\mathbb{E}\{\theta(A \oplus K)\}$:

$$P\{N(K) = n\} = \frac{\mathbb{E}\{\theta(A \oplus K)\}^n}{n!} e^{-\mathbb{E}\{\theta(A \oplus K)\}} \qquad [2.37]$$

This property leads to the following theorem:

THEOREM 2.7.– If the average number of primary grains encountered by K is finite $\mathbb{E}\{\theta(A \oplus K)\} < \infty$, the Choquet capacity of the Boolean model X is written as:

$$T(K) = 1 - e^{-\mathbb{E}\{\theta(A \oplus K)\}} \quad [2.38]$$

for any compact set K included in $\mathbb{R}^d$, where we set:

$$\theta(B) = \int_B \mathrm{d}x\theta(x) \quad [2.39]$$

For a stationary model:

$$T(K) = 1 - e^{-|\theta(A \oplus K)|} \quad [2.40]$$

Finally, for a stationary model of homogeneous intensity:

$$T(K) = 1 - e^{-\theta|A \oplus K|} \quad [2.41]$$

where $|A \oplus K|$ is the mean of the Lebesgue measure of the primary grain A dilated by the compact set K.

The above theorem gives in particular an expression of probability $P\{x \in X\}$.

THEOREM 2.8.– The volume fraction of the stationary Boolean model X of primary grain A and homogeneous intensity θ is written as:

$$T(\{x\}) = P\{x \in X\} = 1 - e^{-\theta|A|} \quad [2.42]$$

The above formula can be demonstrated by elementary means. Let f be the volume fraction of the random set X, a Boolean model of primary grain A and intensity θ. Assume that X is ergodic and denote $\theta = N/V$, where N is the number of grains included in a large size domain V. After adding dN grains, the volume fraction f is changed into $f + \mathrm{d}f$ and the intensity into $\theta + \mathrm{d}\theta$ with $\mathrm{d}\theta = \mathrm{d}N/V$. Now we have on average:

$$\mathrm{d}f = \frac{\mathrm{d}N\,|A|}{V}(1 - f)$$

Indeed, it is clear that $\mathrm{d}f = \mathrm{d}N\,|\,A\,|\,/V$ if $f = 0$ and, on the other hand, if $f > 0$, this value must be weighted by the volume intersected by X^c only, from which the term $1 - f$ is derived. Hence, one has $\mathrm{d}f\,/\,(1-f) = |\,A\,|\,\mathrm{d}\theta$ by integration $1 - f = cste + e^{-|A|\theta}$, the constant being 0.

NOTE.– Theorem [2.42] is also known in crystallization as the Avrami equation (Avrami 1939).

We can demonstrate [2.41] from [2.42]. In effect, one has $1 - T(K) = P\{K \subset X^c\}$. Let K_x be a compact set centered at $x \in \mathbb{R}^d$. Then, we have:

$$K_x \subset X^c \Leftarrow x \in (X^c \ominus K) \Leftarrow x \in (X \oplus K)^c = \bigcup_{y \in \mathcal{P}} [A(y) \oplus K]^c$$

Therefore, K_x is included in the complement of X if and only if x belongs to the complement of the Boolean of germs $\mathcal{P}$ and primary grain $A \oplus K$. We thus exactly obtain formula [2.41].

The volume fraction of X is denoted by $f = P\{x \in X\}$. We can rewrite [2.41] in the form:

$$T(K) = 1 - (1-f)^{|A \oplus K|/|A|} \qquad [2.43]$$

2.4.2. *Properties*

Boolean random sets verify the following fundamental properties:

– Matheron (1975) showed that Boolean models are "infinitely divisible". A random set X is infinitely divisible if, for any integer $n > 0$, X is the union n of Y_i independent random sets $\cup_i Y_i$. This property implies that the union of two realizations of a Boolean model is still Boolean (Serra 1981);

– a section (intersection with a space smaller than d) of a Boolean set is still Boolean (Serra 1983). It should be noted that one cannot generally infer all the characteristics of the model in space $\mathbb{R}^d$ from those obtained in a section. A counterexample is given by a Boolean random set in which some primary grains are

reduced to points. Nevertheless, all the information provided by the functional $T(K)$ can be found when K is itself included in the space of smaller dimension. This includes the volume fraction. For a 3D isotropic model, the covariance is recovered from a section according to a straight line of the model, and thus providing access, for example, to the specific surface;

– Boolean models are stable by dilation. This property is derived from the Choquet capacity formula, where the dilation of a Boolean model of primary grain A by a compact set K is a Boolean model of primary grain $A \oplus K$ (Serra 1981).

Let us examine the "domain of attraction" of the Boolean model. Some limits of unions of random partitions are Boolean models (Serra 1981, 1983; Chiles and Delfiner 2009), in the following sense. Let X be a random partition of $\mathbb{R}^d$ and $\{X_i'\}$ ($i \in \mathcal{I}$) be a family of random sets obtained by choosing each cell of X independently with a probability p, and taking the union closure of the chosen cells.

– We set:

$$Y_n = \bigcup_{i \le n} X_i' \qquad [2.44]$$

We leave $n \to \infty$, $p \to 0$ such that $pn = \theta$ with fixed $0 < \theta < \infty$. Then we show that, for any compact set K:

$$\lim_{n \to \infty} T_n(K) = 1 - e^{-\theta |X'|^{-1} \mathbb{E}\{|X' \oplus K|\}} \qquad [2.45]$$

where X' is the class of the cells of the random partition X and T_n the Choquet capacity associated with Y_n. According to the Choquet–Matheron–Kendall theorem, the limit of Y_∞ of the $(Y_n)_n$ exists and is unique and in addition, Y_∞ is boolean.

NOTE.– The above property shows that Boolean models are obtained as the limit of non-Boolean random partition unions. This property can be seen as a central limit theorem for random sets (Serra 1981; Cressie and Laslett 1987), the union [2.44] of random sets acting as the sum for random variables. This property further suggests that the Boolean model, for random variables, plays an analogous Gaussian-like role for random sets.

2.4.3. *Covariance*

The covariance $C(h)$ of X is calculated using the Choquet capacity. It is written as:

$$C(h) = 2f - 1 + (1-f)^2 e^{\theta|A \cap A_h|} = 2f - 1 + (1-f)^{2-\gamma(h)/\gamma(0)} \quad [2.46]$$

where $\gamma(h) = |A \cap A_h|$ is the geometric covariogram of A.

Simple analytical formulae for the geometric covariogram are known for certain primary grain forms only. For a disc of radius R:

$$\gamma(h) = 2R^2 \left[\cos^{-1}\left(\frac{h}{2R}\right) - \frac{h}{2R}\sqrt{1-\left(\frac{h}{2R}\right)^2} \right] H(2R-h) \quad [2.47]$$

where $H(\cdot) = 1_{\mathbb{R}_+}(\cdot)$ is the Heaviside function. For a sphere of radius R:

$$\gamma(h) = \frac{4\pi R^3}{3}\left(1 - \frac{3h}{4R} + \frac{h^3}{16R^3}\right) H(2R-h) \quad [2.48]$$

Although its definition is very simple, the geometrical covariogram is known only for a few elementary forms, including cylinders of revolution (Gille 1987; Willot 2017), ellipsoids, half-spheres and a few other forms (Gille 2016). It is also known in random forms derived from specific partitions such as Poisson polyhedra (Matheron 1972), cells of a Voronoi partition (Brumberger and Goodisman 1983), or from the typical grain of a dead-leaves pattern (Gille 2002).

2.4.4. *Other characteristics*

2.4.4.1. *Three-point function*

Let $K = \{x, x+h_1, x+h_2\}$, according to [2.41] we have:

$$C(h_1,h_2) = P\{x \in X^c, x+h_1 \in X^c, x+h_2 \in X^c\} = e^{-\theta|A \cup A_{-h1} \cup A_{-h2}|}$$

$$= (1-f)^{3-r(h_1)-r(h_2)+s(h_1,h_2)} \quad [2.49]$$

with:

$$r(h) = \frac{\gamma(h)}{\gamma(0)}, \qquad s(h_1, h_2) = \frac{|\, A \cup A_{-h1} \cup A_{-h2} \,|}{\gamma(0)} \qquad [2.50]$$

Here again, the main difficulty lies in evaluating the functional s for non-trivial primary grain forms.

2.4.4.2. *Contact distribution*

Assume a point x is in the complementary of X and let ℓ be its distance from X. The distribution function of ℓ is given by (Serra 1980):

$$P\{\ell \le L\} = 1 - \frac{1 - T(B_L)}{1 - f} \qquad [2.51]$$

where B_L is the ball of radius L.

2.4.4.3. *Specific surface area*

The specific surface area of a three-dimensional Boolean model X is obtained using [2.12a]:

$$S_V(X) = 4\frac{\gamma'(0)}{\gamma(0)}(1-f)\log(1-f) \qquad [2.52]$$

where $\gamma(h)$ is the geometric covariogram of the primary grain of the model X. We note that $S_V / f \sim cste$ when $f \to 0$, which is expected for grains almost isolated from each other, without interpenetration. On the other hand, $S_v / (1-f) \sim \log(1-f) \to \infty$ in the dual case $f \to 1^-$. Indeed, when $f \to 1$, the Boolean model is composed of a set of very elongated objects that are the (uncovered) interstices between primary grains, and these interstices have a surface/volume ratio that becomes infinite.

2.4.4.4. *Linear erosion curves for convex primary grains*

Assume that A is a convex random compact set. Steiner's formula [2.19] allows us to explicitly calculate $T(K)$. The measure of $A \oplus \lambda K$ is in particular a polynomial of degrees d in λ, whose coefficients depend on the Minkowski functionals of A. If, for example, $K = [x; x+h]$ is a segment of length h and

orientation, $|A \oplus K| = |A| + h|A_\alpha|$, where A_α represents the length of the boundary of A in the direction of dilation α. The probability P_X^c that a segment L of length h is included in the complement of the Boolean model is then (see equation [2.22]):

$$\begin{aligned} P_X^c(h) &= P\left\{L \subset X^c\right\} = e^{-\theta|A\oplus K|} = e^{-\theta\left(|A|+h|A_\alpha|\right)} \\ &= e^{-\theta\left[\gamma(0)-h\gamma'(0)\right]} = \left(1-f\right)^{1-h\gamma'(0)/\gamma(0)} \end{aligned} \qquad [2.53]$$

This relation is particularly useful because it allows testing the validity of the Boolean assumption: *for any convex primary grain, the linear erosion curve of a Boolean model varies exponentially with the length*.

NOTE.– By taking a Cox process as a set of germs, itself based on a Boolean model, multiscale structures can be generated (see, for example, Jean *et al.* 2011).

An upper bound on the length of the minimum path length going through a Boolean medium of uniform intensity having disks or squares ($d = 2$) or hyperspheres ($d \geq 2$) as the primary grain was calculated by Willot (2015) for a diluted volume fraction ($f \ll 1$).

This bound shows non-trivial exponents ($\sim f^{2/3}$ for $d = 2$, for $\sim f^{1/2}$ $d = 3$), and a diameter-dependent prefactor in the direction of propagation of the primary grain.

Doi (1976) calculated the surface correlation functions of a three-dimensional Boolean model of spheres. For a random set X, these correlation functions are defined by the quantities:

$$F_{sv}(x_1, x_2) = \langle \chi(x_1) s(x_2) \rangle \qquad [2.54a]$$

$$F_{ss}(x_1, x_2) = \langle s(x_1) s(x_2) \rangle \qquad [2.54b]$$

with $\chi(\cdot)$ with the indicator of X, $1-\chi(\cdot)$ that of X^c and:

$$s(x) = |\nabla \chi(x)| \qquad [2.55]$$

where ∇ is the nabla vector-operator of components $\partial / \partial x_i$ ($i = 1, ..., d$), x_i being the ith component of x in a Cartesian coordinate system. For a stationary random

set, the correlation functions F_{ss} and F_{sv} depend only on $x_1 - x_2$, and only on $h = |x_1 - x_2|$ for an isotropic model.

We also have, when $h \to \infty$ (Torquato 2013):

$$F_{sv}(h) \sim fs, \qquad F_{ss}(h) \sim s^2, \quad r \to \infty \tag{2.56}$$

where s is the specific surface area of ∂X.

Torquato (2013) gives for the Boolean sphere model, in dimension 3:

$$F_{sv}(r) = \frac{-3\log(1-f)}{R}\left[2 - \frac{\gamma(h)}{\gamma(0)}\right]\left[1 - \left(\frac{1}{2} - \frac{h}{4R}\right)H(2R-h)\right] \tag{2.57a}$$

$$F_{ss}(r) = \left[2 - \frac{\gamma(h)}{\gamma(0)}\right]\left\{\frac{9\log^2(1-f)}{R^2}\left[1 - \left(\frac{1}{2} - \frac{h}{4R}\right)H(2R-h)\right]^2 - \frac{3\log(1-f)}{2hR}H(2R-h)\right\} \tag{2.57b}$$

The functions F_{sv} and F_{sv} appear in particular in the expressions of certain bounds of the permeability of porous media (Doi 1976; Berryman and Milton 1985; Willot *et al.* 2016; Bignonnet 2018).

2.5. RSA models

The random sequential adsorption (RSA) model (Talbot *et al.* 2000) is a model in which, unlike the Boolean model, grains are added sequentially by prohibiting interpenetration. In the simplest case, the intensity is taken uniformly in R^d. When a grain partially overlaps a grain previously positioned, it is rejected (see Månsson and Rudemo (2002) for other disjoint grain models). Few exact results are known for the RSA model, except in the one-dimensional case (Torquato 1995).

For a small volume fraction of the random set, the RSA model is asymptotically equal to a Boolean medium and the grain positions are those of a Poisson point process (Månsson and Rudemo 2002). The RSA model does not allow high-density realizations to be generated. In this case, special techniques must be implemented, in which objects are placed and restoring forces are imposed between interpenetrating objects. This approach was proposed in particular for the modeling of fibrous media (Altendorf and Jeulin 2011).

The images in Figure 2.3(a) show two-dimensional, cross-sections following two orthogonal directions, of a composite material, and Figure 2.3(b) shows a random fiber model reproducing the microstructure characteristics, with in particular the radius of curvature of the fibers and their tortuosity.

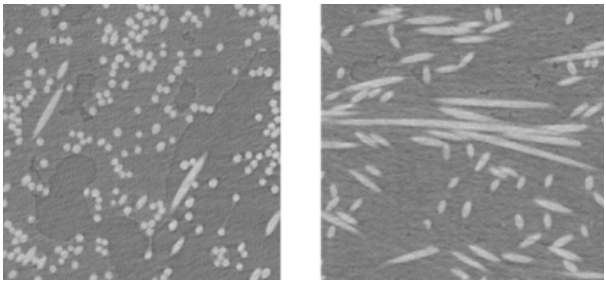

a)

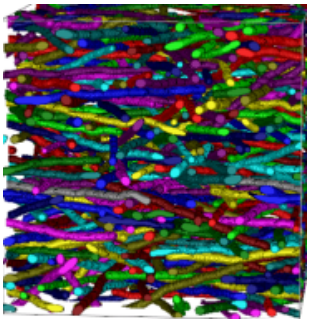

b)

Figure 2.3. *(a) Composite fibrous medium; (b) model (source: taken from Altendorf et al. 2014)). For a color version of this figure, see www.iste.co.uk/gogu/uncertainties.zip*

2.6. Random tessellations

A random tessellation or partition of space is by definition a set of pairwise disjoint bounded open subsets (cells) of $\mathbb{R}^d$ and whose union closure covers the whole space. Matheron (1969) showed that probabilities could be defined on a σ-algebra defined based on such tessellations of $\mathbb{R}^d$ to which the set of points located at the edges of the cells is added (see Lantuéjoul 2002).

Two approaches are possible to calculate properties relating to grain characteristics (number of neighbors, average surface area, etc.). In the first case, the focus is on the cell containing the origin (there is one with probability 1), called the *fundamental cell*. In the second approach, the distribution of a characteristic is calculated from all the cells of all the realizations, or from all the cells of a realization of an ergodic model. Although no particular cell has been chosen, it is referred to as *typical cell* in this case. In the first case, which is a volume distribution, large volume cells will be more represented than in the second case, which consists of calculating a number distribution.

In all the following examples, it is assumed that the number of cells intersected by a compact set is finite with probability 1.

2.6.1. *Voronoi tessellation*

The Poisson–Voronoi tessellation is defined by influence zones $C(g,X)$ of the germs g of a Poisson point model $\mathcal{P}$. The cell $C(g,X)$ associated with the germ $g \in \mathcal{P}$ is:

$$C(g,X) = \{x \in \mathbb{R}^d : \ |x-g| < |x-g'| \forall g' \in \mathcal{P}, g' \neq g\} \quad [2.58]$$

This cell is a convex polytope delimited by parts of hyperplanes. Despite the simplicity of the model, the analytical results from the Voronoi model are limited. In three dimensions, the volume distribution of the surface of the typical cell C_t is known, whose mean is written as (Miles 1974; Møller 1989):

$$\mathbb{E}\{|\partial C_t|\} = \frac{2\sqrt{\pi}(d-1)!\Gamma(1+d/2)^{1-1/d}\Gamma(2-1/d)}{\theta^{1-1/d}\Gamma((d+1)/2)\Gamma(d-1/2)} \quad [2.59]$$

where $\Gamma(\cdot)$ is the extension of the factorial function to $\mathbb{R}$ $\Gamma(n) = (n-1)!$ (n being an integer). Similar results are known for the mean lengths of the triple lines of the typical grain, and more generally for the d'-volumes of dimension $d' < d$ of the d'-facets of the typical cell of the Voronoi tessellation of dimension d.

The *number* distribution of the area or volume of Voronoi cells is often modeled, in an approximate way, by gamma distributions (Ferenc and Néda 2007; Farjas and Roura 2008); this result being exact in dimension 1. It should be noted that the 2D section of a 3D Voronoi tessellation is not a two-dimensional Voronoi tessellation. The latter presents in particular distributions of distinct cell sizes.

The distribution of the number of sides in the typical cell of a two-dimensional Voronoi partition was calculated by Calka (2003a). The same author studied the distribution of the area and perimeter of the same cell (Calka 2003b) and other quantities related in particular to the size of the largest disk included in the typical cell, which has a point in the cell as its center (Calka 2002).

2.6.2. *Johnson–Mehl tessellation*

A Johnson–Mehl tessellation is defined by a Poisson points process in $\mathbb{R}^d \times \mathbb{R}_+$, the last dimension being a time dimension. Germs g_i ($i = 1, ..., N$) are implanted sequentially at times t_i ($i = 1, ..., N$). The associated classes $C(g_i, X)$ are given by:

$$C(g_i, X) = \{x \in \mathbb{R}^d : \; t_i + \frac{|x - g_i|}{v} < t_j + \frac{|x - g_j|}{v} \forall j \neq i, \} \qquad [2.60]$$

where v *is* a velocity of propagation of the edge cells. A different choice of v is equivalent to changing the spatial scale and does not fundamentally alters the model. The Johnson–Mehl model is perhaps the simplest random partition with non-convex grains.

2.6.3. *Laguerre tessellation*

Poisson–Voronoi and Poisson–Johnson–Mehl random tessellations depend essentially on one parameter, the intensity of the Poisson point process, which is a scaling factor and only trivially modifies the resulting structure. In many applications, it is desirable to generate random partitions with a prescribed distribution of a geometric characteristic of the cells. For example, consider the number-weighted distribution of the volume of cells. Each grain must then be assigned a weight representative of the characteristics of the grain.

Given a process of random Poisson points g_i, the Laguerre tessellation consists of dividing $\mathbb{R}^d$ into cells defined as:

$$C(g_i, X) = \{x \in \mathbb{R}^d : \; |x - g_i|^2 - r_i^2 < |x - g_j|^2 - r_j^2 \; \forall j \neq i, \} \qquad [2.61]$$

where r_i are positive weights assigned to each germ, which follow a certain distribution $\mathcal{R}$. Similarly to the Voronoi tessellation, the cells of a Laguerre tessellation are convex polytopes; however, unlike the Voronoi model, some cells

may be empty, and some may not contain their germ. The Laguerre model offers extra degrees of freedom compared to the Voronoi tessellation. The distribution of size $\mathcal{R}$ can be adjusted to simulate cells with volume distributions much more widely spread out than the random Voronoi tessellation (Lautensack and Zuyev 2008), which makes it possible to model cellular media or foams (Redenbach 2009), or even polycrystals.

2.6.4. *Random Poisson tessellation*

A Poisson tessellation is defined by a set of hyperplanes in $\mathbb{R}^d$. Each hyperplane is parameterized by its distance from the origin and a direction in the half-hypersphere S_d^+. The model can thus be seen as a Poisson process in $\mathbb{R}^d \times S_d^+$. Thereby, it is completely determined by a single parameter, the intensity θ of the Poisson point process. The cells of the Poisson random tessellation are the subsets of $\mathbb{R}^d$ delimited by the boundaries of the Poisson hyperplanes.

A large number of exact results are available for the typical polytope of the Poisson partition. Miles (1964, 1974) calculated its average perimeter ($d = 2$), the average number of vertices, the average total length of its edges, and its average area ($d = 3$). In general, for the volume $F_{d'}$ of the $d' \leq d$ -dimension variety of the typical polytope C_t:

$$\mathbb{E}\{F_{d'}\} = \binom{d}{d'} \frac{2^d}{\omega_{d'}(\omega_{d-1}\theta)^{d'}} \qquad [2.62]$$

Matheron (1975) gives the mean value of the Minkowski function of C_t:

$$\mathbb{E}\{W_i(C_t)\} = \frac{\omega_i}{\omega_{d-i}} \left(\frac{2}{\omega_{d-1}\theta} \right)^{d-i}, \qquad 0 \leq i \leq d \qquad [2.63]$$

Miles (1974) gives the average number $N_{d'}$ of the d'-face ($d' \leq d$ -dimensional variety) of the typical cell C_t:

$$\mathbb{E}\{N_{d'}\} = 2^{d-d'} \binom{d}{d'} \qquad [2.64]$$

In addition, it is shown that the random partition obtained by intersection of a Poisson partition in $\mathbb{R}^d$ by a dimensional hyperplane d' is still a Poisson partition in $\mathbb{R}^{d'}$. Its intensity is written as (Miles 1964):

$$\theta' = \frac{\omega_{d-1}}{\omega_{d'-1}}\theta \qquad [2.65]$$

The first three moments of the volume distribution of the fundamental cell C_f of the Poisson partition were obtained by Matheron (1975). Its mean is more specifically written as:

$$\mathbb{E}\{|C_f|\} = \frac{d!\omega_d}{(\omega_{d-1}\theta)^d} \qquad [2.66]$$

Poisson random partition models have been used in particular to model the granulometries obtained by screening concrete aggregates (Escoda *et al.* 2015) or to simulate cementitious materials (Heinemann *et al.* 1999). On the other hand, these cells can be used as random primary grains of Boolean models, for example to represent tungsten carbides (Quénec'h *et al.* 1996).

2.6.5. *The dead-leaves model*

The dead-leaves model was originally introduced by Matheron (1968) and extended by Jeulin (1979) (see also Serra 1983). It is a sequential Boolean model that asymptotically fills up the whole space and defines a random partition. It makes use of n "colors" indexed by an integer $i \in \mathcal{I}$. The "leaves" are random compacts sets of $\mathbb{R}^d$, which appear at times $-\infty < t < 0$, according to a Poisson point process of intensity θ in $\mathbb{R}^d \times \mathbb{R}_-$. Each leaf is assigned a color in $\mathcal{I}$ independently of the color of the other leaves. The colored leaves i appear in the time interval $[t; t+\mathrm{d}t]$ with a probability p_i. Those that appear in the time interval $[t; t+\mathrm{d}t]$ form a Boolean model where the random compact set A_i is the primary grain. The grain that appeared in x at time t is denoted by $A(x,t)$. The grains cover those that appeared previously.

At time $t = 0$, the space $\mathbb{R}^d$ is covered at every point by a grain with a probability of 1. The random partition is formed by uncovered cells $A(x,t)$. These are additionally identified by a color in I. The cells are in general not connected.

We know how to calculate for this model the probability that each point y_i in a finite set of points $Y \subset \mathbb{R}^d$ is of a given color, depending on y_i (Lantuéjoul 2002). In particular, we have access to the two-point spatial distribution, which is written using the Lantuéjoul (2002) notations:

$$P\{Z(x)=i, Z(y)=j\} = \frac{a_i(a_j - b_j) + a_j(a_i - b_i) + ab_i\delta_{ij}}{a(2a-b)} \quad [2.67]$$

where δ_{ij} is the Kronecker symbol, $Z(x)$ is the color of the partition at point x at the time $t = 0$ and:

$$a_i = \theta p_i \mathbb{E}\{|A_i|\}, \quad b_i = \theta p_i K_i(x-y), \quad a = \sum_i a_i, \quad b = \sum_i b_i \quad [2.68]$$

with $K_i(\cdot)$ the geometric covariogram of A_i:

$$\mathbb{E}\left\{\left|\left(A_i \ominus \{x,y\}\right) \setminus \left(A_i \oplus \{x\}\right)\right|\right\} = K_i(0) - K_i(x-y) \quad [2.69]$$

The dead-leaves model is often used to model occlusion phenomena in natural images (Lee *et al.* 2001), or to analyze two-dimensional images obtained by electron microscopy, powders for example (Jeulin *et al.* 1995). Furthermore, the set of intact grains at $t = 0$ is an interesting random model for generating high-density stacks, if the intensities and grains are properly chosen over time (Jeulin 2019).

2.6.6. *Generalized random partition models*

Random partitions based on Poisson point processes can be generalized using local metrics (not necessarily Euclidean) attached to each germ (Jeulin 2013) and reinterpreted from Boolean function models. Figure 2.4(a) shows an example of a non-convex grain random partition (Gasnier *et al.* 2015a), obtained from a generalized Johnson–Mehl model with an anisotropic distance. The latter models a polycrystal whose grain boundaries, seen by scanning electron microscopy (SEM), have been separated from their backgrounds (see Figure 2.4(b)). The model is three dimensional, and the SEM image is two dimensional. The cell shapes in the Johnson–Mehl model with an anisotropic distance are more elongated than in the classical Johnson–Mehl model. The model is macroscopically isotropic.

Figliuzzi (2019) proposes an approach enabling grain interfaces to be generated with controlled roughness and a method for the rapid simulation of random partitions on a voxel grid.

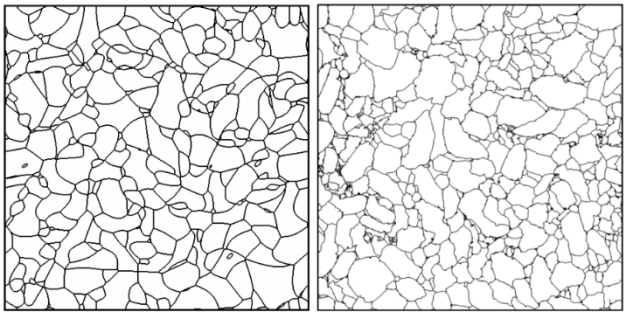

a) b)

Figure 2.4. *(a) Two-dimensional section of a Johson–Mehl random partition modeling a polycrystal; (b) segmented experimental image (source: image (a) from Gasnier et al. 2015b); image (b) from Philippe Lambert/CEA le Ripault)*

2.7. Gaussian fields

In this section, we briefly define Gaussian random functions as well as Gaussian excursions, and describe how they may be simulated. The theory of Gaussian functions was originally studied by Rice (1944) in the one-dimensional case and by Longuet-Higgins (1957) in two-dimensional case. Bardeen *et al.* (1985) define a Gaussian random function as a function whose n-point distribution laws are multivariate Gaussian.

Gaussian excursion models allow one to simulate microstructures having a fixed covariance function. The covariance, in fact, fully determines the Gaussian random function. The remainder of this section explains how to generate such a model. For a detailed description of Gaussian random functions, see Lantuéjoul (1994, 2002).

Let $U(x)$ be a Gaussian noise, namely such that $U(x)$ is a normal distribution for all x and $U(x)$, $U(x')$ are independent if $x \neq x'$.

We consider the random function $Z(x)$ and the random set X:

$$X = \left\{ x \in \mathbb{R}^d ; Z(x) \geq \lambda \right\} \quad [2.70a]$$

$$Z(x) = (w * U)(x), \qquad U(x) \sim \mathcal{N}(0,1) \quad [2.70b]$$

where w is a weight function, λ a scalar, designates a convolution product, and $\mathcal{N}(0,1)$ is the normal distribution of zero mean and variance 1. The mean of the indicator function of X is equal to:

$$f = P\{Z(x) \geq \lambda\} = P\{\mathcal{N}(0,1) \geq \lambda\} \quad [2.71]$$

which determines λ according to f:

$$\lambda = F^{-1}(1-f) \quad [2.72]$$

where F is the cumulative distribution function of the normal distribution.

The weight function w verifies:

$$\int_{\Omega} w^2(x)\mathrm{d}x = 1, \qquad w(x) = w(-x) \quad [2.73]$$

This is related to the covariance $C(h)$ by X (Bron and Jeulin 2011):

$$C(h) = \frac{1}{2\pi} \int_0^{\rho(h)} \frac{1}{\sqrt{1-t^2}} e^{\frac{-\lambda^2}{1+t}} \mathrm{d}t \quad [2.74]$$

where $\rho_X(h) = (w * w)(h)$.

The function w is obtained by means of:

$$w = FT^{-1}\left\{ \sqrt{FT\{\rho\}} \right\} \quad [2.75]$$

where FT and FT^{-1} are the direct and inverse Fourier transforms in $\mathbb{R}^d$. Once λ is calculated, the function ρ is obtained by numerically inverting [2.74] and w is given by [2.75].

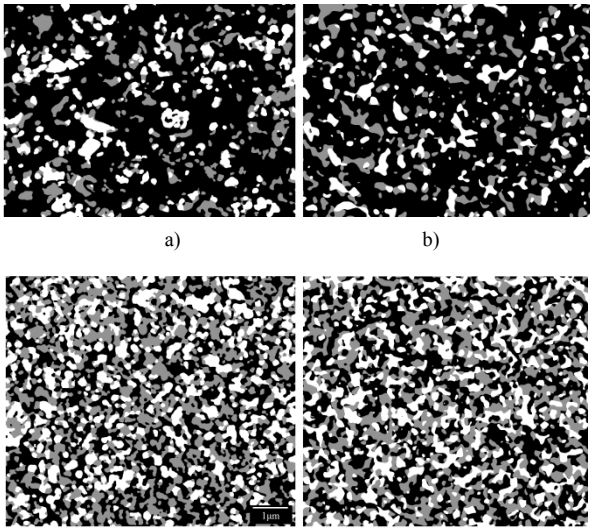

Figure 2.5. *(a and c) SEM image (after segmentation) of fuel cell anode layers; (b and d) plurigaussian model (source: from Abdallah et al. 2015)*

A model based on Gaussian excursions is developed by Abdallah *et al*. (2015) (see Figure 2.5). To simulate a three-phase random medium, it is assumed that there are two independent random sets X and Y such that one of the phases is given by X, another by $Y \setminus X$ and the third by the complementary of the union of the other two. Due to the independence of the random sets X and Y, the cross-covariance C_{12} of the phases 1 and 2 is given by the covariances C_1 and C_2 of these same phases. In effect:

$$C_{12}(h) = P\{x \in phase(1); x+h \in phase(2)\} = \frac{C_2(0)[C_1(0) - C_1(h)]}{1 - C_1(0)} \quad [2.76]$$

This property allows one to test whether modeling using independent sets X and Y is possible, regardless of the choice of X and Y. Moreover, the covariances of X and Y can be calculated from those of phases 1 and 2. Figure 2.5 represents the results obtained in the case of Gaussian excursions for X and Y. This model is used to represent the microstructure of anode layers consisting of two solid phases and a porous phase, existing in some fuel cells and for which only two-dimensional

representations are known. The model has been compared to a graph-based approach (Neumann *et al.* 2019).

2.8. Conclusion

In this chapter, we have presented some of the most commonly used random models. They are parsimonious in the sense that they are defined by few parameters. In general, they can be easily simulated and, in some cases, analytical results are available. They can be directly used to model a particular microstructure or combined with one another to generate sets representative of microstructures, especially multiscale structures (an example of such combination is shown in Figure 2.6). Nevertheless, numerical calculations and simulations, not discussed in this chapter, are often necessary to accurately represent real microstructures.

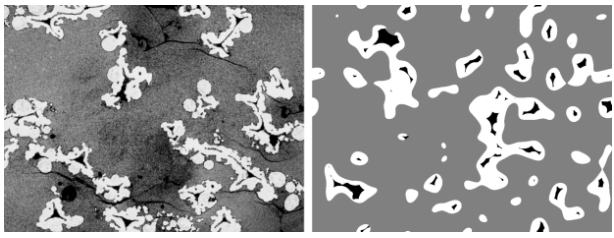

a) b)

Figure 2.6. *(a) SEM image of a fuel cell foam; (b) realization of a "Boolean random shell model" (source: from Abdallah (2015), image (a) from A. Chesnaud/Mines ParisTech)*

The main difficulty with these approaches lies in the determination of the relevant morphological criteria and the choice of a model. To illustrate this problem, one can refer to Figure 2.7, which represents three isotropic microstructures with the same covariance and same three-point functions (Chilès and Lantuéjoul 2005). This example illustrates the extent to which the covariances and even the trivariate functions remain "blind" and do not allow us to distinguish geometries that are very different from one another. Within the context of random set approaches, the issue surrounding the choice of model remains an open problem.

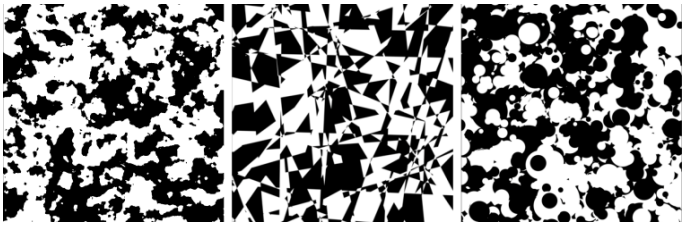

a) b) c)

Figure 2.7. *Random realizations of three probabilistic models with the same trivariate function: (a) Gaussian excursion; (b) random Poisson partition; (c) dead-leaves model (source: from Chilès and Lantuéjoul 2005)*

2.9. Acknowledgments

The author thanks C. Lantuéjoul for the images in Figure 2.7, H. Trumel for the image in Figure 2.4(b), C. Gogu and Delphine Livet for their proofreading work and G. Moreira for translating this text into English.

2.10. References

Abdallah, B. (2015). Analyse morphologique et modélisation pour l'optimisation structurelle d'électrodes. PhD Thesis, École nationale supérieure des mines, Paris.

Abdallah, B., Willot, F., Jeulin, D. (2015). Stokes flow through a Boolean model of spheres: Representative volume element. *Transport in Porous Media*, 109(3), 711–726.

Altendorf, H., Jeulin, D. (2011). Random-walk-based stochastic modeling of three-dimensional fiber systems. *Physical Review E*, 83(4), 041804.

Altendorf, H., Jeulin, D., Willot, F. (2014). Influence of the fiber geometry on the macroscopic elastic and thermal properties. *International Journal of Solids and Structures*, 51(23), 3807–3822.

Angulo, J. (2012). Morphologie mathématique pour des images multi-variées. PhD Thesis, Université Paris-Est, Marne-la-Vallée.

Avrami, M. (1939). Kinetics of phase change. I general theory. *The Journal of Chemical Physics*, 7(12), 1103–1112.

Azzimonti, D., Willot, F., Jeulin, D. (2013). Optical properties of deposit models for paint: Full-fields FFT computations and representative volume element. *Journal of Modern Optics*, 60(7), 519–528.

Bardeen, J., Szalay, A., Kaiser, N., Bond, J. (1985). The statistics of peaks of Gaussian random fields. *The Astrophysical Journal*, 304, 15–61.

Berryman, J., Milton, G. (1985). Normalization constraint for variational bounds on fluid permeability. *The Journal of Chemical Physics*, 83(2), 754–760.

Bignonnet, F. (2018). Upper bounds on the permeability of random porous media. *Transport in Porous Media*, 122(1), 57–76.

Bochner, S. (1959). *Lectures on Fourier Integrals*. Princeton University Press, Princeton.

Bortolussi, V., Figliuzzi, B., Willot, F., Faessel, M., Jeandin, M. (2018). Morphological modeling of cold spray coatings. *Image Analysis and Stereology*, 37(2), 145–158.

Bron, F., Jeulin, D. (2011). Modelling a food microstructure by random sets. *Image Analysis and Stereology*, 23(1), 33–44.

Brumberger, H., Goodisman, J. (1983). Voronoï cells: An interesting and potentially useful cell model for interpreting the small-angle scattering of catalysts. *Journal of Applied Crystallography*, 16(1), 83–88.

Calka, P. (2002). The distributions of the smallest disks containing the Poisson-Voronoï typical cell and the Crofton cell in the plane. *Advances in Applied Probability*, 34(4), 702–717.

Calka, P. (2003a). An explicit expression for the distribution of the number of sides of the typical Poisson-Voronoï cell. *Advances in Applied Probability*, 35(4), 863–870.

Calka, P. (2003b). Precise formulae for the distributions of the principal geometric characteristics of the typical cells of a two-dimensional Poisson-Voronoï tessellation and a Poisson line process. *Advances in Applied Probability*, 35(3), 551–562.

Chilès, J.-P., Delfiner, P. (2009). *Geostatistics: Modeling Spatial Uncertainty*. John Wiley & Sons, New York.

Chilès, J.-P., Lantuéjoul, C. (2005). Prediction by conditional simulation. In *Space, Structure and Randomness. Contributions in Honor of Georges Matheron in the Fields of Geostatistics, Random Sets and Mathematical Morphology*, Bilodeau, M., Meyer, F., Schmitt, M. (eds). Springer, New York, 39–68.

Choquet, G. (1954). Theory of capacities. *Annales de l'Institut Fourier*, 5, 131–295.

Christakos, G. (1984). On the problem of permissible covariance and variogram models. *Water Resources Research*, 20(2), 251–265.

Cressie, N., Laslett, G.M. (1987). Random set theory and problems of modeling. *SIAM Review*, 29(4), 557–574.

Daley, D.J., Vere-Jones, D. (1988). *An Introduction to the Theory of Point Processes Springer Series in Statistics*. Springer-Verlag, New York.

Doi, M. (1976). A new variational approach to the diffusion and the flow problem in porous media. *Journal of the Physical Society of Japan*, 40(2), 567–572.

Emery, X., Lantuéjoul, C. (2011). Geometric covariograms, indicator variograms and boundaries of planar closed sets. *Mathematical Geosciences*, 43(8), 905–927.

Escoda, J. (2012). Modélisation morphologique et micromécanique 3D de matériaux cimentaires. Thèse de doctorat, École nationale supérieure des mines, Paris.

Escoda, J., Jeulin, D., Willot, F., Toulemonde, C. (2015). 3D morphological modeling of concrete using multiscale Poisson polyhedra. *Journal of Microscopy*, 258(1), 31–48.

Farjas, J., Roura, P. (2008). Cell size distribution in a random tessellation of space governed by the Kolmogorov-Johnson-Mehl-Avrami model: Grain size distribution in crystallization. *Physical Review B*, 78(14), 144101.

Ferenc, J.-S., Néda, Z. (2007). On the size distribution of Poisson Voronoi cells. *Physica A: Statistical Mechanics and its Applications*, 385(2), 518–526.

Figliuzzi, B. (2019). Eikonal-based models of random tesselations. *Image Analysis and Stereology*, 38(1), 15–23.

Gasnier, J., Figliuzzi, B., Faessel, M., Willot, F., Jeulin, D., Trumel, H. (2015a). 3D morphological modeling of a polycrystaline microstructure with non-convex, anisotropic grains [Online]. In *Acta Stereologica*. *Proceedings of the 14th International Congress for Stereology and Image Analysis (ICSIA)*. Liège, 7-10 July. Available at: https://hal.archives-ouvertes.fr/hal-01184811.

Gasnier, J., Willot, F., Trumel, H., Figliuzzi, B., Jeulin, D., Biessy, M. (2015b). A Fourier-based numerical homogenization tool for an explosive material. *Matériaux et techniques*, 103(3), 308.

Gille, W. (1987). The intercept length distribution density of a cylinder of revolution. *Experimentelle Technik der Physik*, 35(2), 93–98.

Gille, W. (2002). The set covariance of a dead leaves model. *Advances in Applied Probability*, 34(1), 11–20.

Gille, W. (2016). *Particle and Particle Systems Characterization: Small-Angle Scattering (SAS) Applications*. CRC Press, Boca Raton.

Greco, A., Jeulin, D., Serra, J. (1979). The use of the texture analyser to study sinter structure: application to the morphology of calcium ferrites encountered in basic sinters of rich iron ores. *Journal of Microscopy*, 116(2), 199–211.

Hadwiger, H. (1957). Über eibereiche mit gemeinsamer treffgeraden. *Portugaliae mathematica*, 16(1), 23–29.

Heinemann, A., Hermann, H., Wetzig, K., Häussler, F., Baumbach, H., Kröning, M. (1999). Fractal microstructures in hydrating cement paste. *Journal of Materials Science Letters*, 18(17), 1413–1416.

Heinrich, L. (1992). On existence and mixing properties of germ-grain models. *Statistics*, 23(3), 271–286.

Jean, A., Jeulin, D., Forest, S., Cantournet, S., N'Guyen, F. (2011). A multiscale microstructure model of carbon black distribution in rubber. *Journal of Microscopy*, 241(3), 243–260.

Jeulin, D. (1979). Morphologie mathématique et propriétés physiques des agglomérés de minerais de fer et du coke métallurgique. PhD Thesis, École nationale supérieure des mines de Paris.

Jeulin, D. (2013). Random tessellations and Boolean random functions. In *Mathematical Morphology and Its Applications to Signal and Image Processing*, Luengo Hendriks, C.L., Borgefors, G., Strand, R. (eds). Springer, Berlin, 25–36.

Jeulin, D. (2016). Power laws variance scaling of Boolean random varieties. *Methodology and Computing in Applied Probability*, 18(4), 1065–1079.

Jeulin, D. (2019). Some dense random packings generated by the dead leaves model. *Image Analysis and Stereology*, 38(1), 3–13.

Jeulin, D., Ostoja-Starzewski, M. (2001). *Mechanics of Random and Multiscale Microstructures*. Springer, Berlin.

Jeulin, D., Villalobos, I.T., Dubus, A. (1995). Morphological analysis of UO, powder using a dead leaves model. *Microscopy Microanalysis Microstructures*, 6(4), 371–384.

Kendall, D. (1974). Foundations of a theory of random sets. In *Stochastic Geometry: A Tribute to the Memory of Rollo Davidson*, Harding, E.F., Kendall, D.G. (eds). Wiley, London.

Lantuéjoul, C. (1991). Ergodicity and integral range. *Journal of Microscopy*, 161(3), 387–403.

Lantuéjoul, C. (1994). Non conditional simulation of stationary isotropic multi-Gaussian random functions. In *Geostatistical Simulations*, Armstrong, M., Dowd, P.A. (eds). Springer, Berlin, 147–177.

Lantuéjoul, C. (2002). *Geostatistical Simulation: Models and Algorithms*. Springer, Berlin.

Lautensack, C., Zuyev, S. (2008). Random Laguerre tessellations. *Advances in Applied Probability*, 40(3), 630–650.

Lee, A., Mumford, D., Huang, J. (2001). Occlusion models for natural images: A statistical study of a scale-invariant dead leaves model. *International Journal of Computer Vision*, 41(1–2), 35–59.

Månsson, M., Rudemo, M. (2002). Random patterns of nonoverlapping convex grains. *Advances in Applied Probability*, 34(4), 718–738.

Matheron, G. (1965). *Les variables régionalisées et leur estimation: une application de la théorie des fonctions aléatoires aux sciences de la nature*. Masson, Paris.

Matheron, G. (1967). *Éléments pour une théorie des milieux poreux*. Masson, Paris.

Matheron, G. (1968). Schéma booléen séquentiel de partition aléatoire. Rapport technique N-83, Centre de morphologie mathématique, École nationale supérieure des Mines, Paris. [Online]. Available at: http://cg.ensmp.fr/bibliotheque/public/MATHERON_Rapport_00121.pdf.

Matheron, G. (1969). *Théorie des ensembles aléatoires*. École nationale supérieure des Mines, Paris.

Matheron, G. (1972). Ensembles fermés aléatoires, ensembles semi-markoviens et polyèdres poissoniens. *Advances in Applied Probability*, 4(3), 508–541.

Matheron, G. (1975). *Random Sets and Integral Geometry*. Wiley, New York.

Matheron, G. (1989a). *Estimating and Choosing: An Essay on Probability in Practice*. Springer, Berlin.

Matheron, G. (1989b). The internal consistency of models in geostatistics. In: *Geostatistics*, Armstrong, M. (ed.). Springer, Dordrecht, 21–38.

Matheron, G., Serra, J. (1982). *Image Analysis and Mathematical Morphology*. Academic Press, London.

Miles, R.E. (1964). Random polytopes: The generalisation to n dimensions of the intervals of a Poisson process. PhD Thesis, Université de Cambridge, Cambridge.

Miles, R.E. (1974). A synopsis of "Poisson flats in Euclidean spaces". *Stochastic Geometry*, 202–227.

Milton, G.W. (2002). *The Theory of Composites*. Cambridge University Press, Cambridge.

Molchanov, I.S. (2005). *Theory of Random Sets*. Springer, Berlin.

Møller, J. (1989). Random tessellations in R^d. *Advances in Applied Probability*, 21(1), 37–73.

Neumann, M., Abdallah, B., Holzer, L., Willot, F., Schmidt, V. (2019). Stochastic 3D modeling of three-phase microstructures for the prediction of transport properties in solid oxide fuel cells. *Transport in Porous Media*, 128(1), 179–200.

Quénec'h, J.-L., Chermant, J.-L., Coster, M., Jeulin, D. (1996). Example of application of probabilistic models: Determination of the kinetics parameters during liquid phase sintering. *Microscopy Microanalysis Microstructures*, 7(5–6), 573–580.

Redenbach, C. (2009). Microstructure models for cellular materials. *Computational Materials Science*, 44(4), 1397–1407.

Redenbach, C., Wirjadi, O., Rief, S., Wiegmann, A. (2011). Modeling a ceramic foam for filtration simulation. *Advanced Engineering Materials*, 13(3), 171–177.

Rice, S.O. (1944). Mathematical analysis of random noise. *Bell System Technical Journal*, 23(3), 282–332.

Schneider, R., Weil, W. (2008). *Stochastic and Integral Geometry*. Springer-Verlag, Berlin, Heidelberg.

Serra, J. (1980). The Boolean model and random sets. *Computer Graphics and Image Processing*, 12(2), 99–126.

Serra, J. (1981). The Boolean model and random sets. In: *Image Modeling*, Rosenfield, A. (ed.). Academic Press, Cambridge, 343–370.

Serra, J. (1983). *Image Analysis and Mathematical Morphology*. Academic Press, Cambridge.

Stroeven, P. (2000). A stereological approach to roughness of fracture surfaces and tortuosity of transport paths in concrete. *Cement and Concrete Composites*, 22(5), 331–341.

Talbot, J., Tarjus, G., Van Tassel, P., Viot, P. (2000). From car parking to protein adsorption: An overview of sequential adsorption processes. *Colloids and Surfaces A: Physico-chemical and Engineering Aspects*, 165(1–3), 287–324.

Torquato, S. (1995). Nearest-neighbor statistics for packings of hard spheres and disks. *Physical Review E*, 51(4), 3170.

Torquato, S. (2013). *Random Heterogeneous Materials: Microstructure and Macroscopic properties*. Springer, Berlin.

Van Lieshout, M. (2000). *Markov Point Processes and Their Applications*. Imperial College Press, London.

Willot, F. (2015). The power laws of geodesics in some random sets with dilute concentration of inclusions. *Lecture Notes in Computer Science*, 9082, 535–546.

Willot, F. (2017). Mean covariogram of cylinders and applications to Boolean random sets. *Journal of Contemporary Mathematical Analysis*, 52(6), 305–315.

Willot, F., Jeulin, D. (2011). Elastic and electrical behavior of some random multiscale highly-contrasted composites. *International Journal for Multiscale Computational Engineering*, 9(3), 305–326.

Willot, F., Abdallah, B., Jeulin, D. (2016). The permeability of Boolean sets of cylinders. *Oil and Gas Science and Technology*, 71(2).